Mateusz ZAPART[1], Cezary WOREK[1]

AGH University of Science and Technology, Institute of Electronics (1)
ORCID.

doi:10.15199/48.2022.02.22

Design and simulations of medium frequency power supply for plasma processing and magnetron sputtering

Streszczenie. *W artykule przedstawiono, przetwornicę z obwodem rezonansowym 4 rzędu typu LCLC, pracującą na częstotliwościach około 100 kHz przeznaczoną do zasilana magnetronu. Ta nietypowa topologia charakteryzuje się wyjściem o charakterze źródła prądowego z możliwością osiągnięcia wysokiego napięcia bez obciążenia, co jest zaletą w przypadku zasilania procesów plazmowych. Wiąże się również z mniejszymi wymaganiami dotyczącymi szybkości kontrolera, co pozwala na realizację cyfrowych pętli sprzężenia z wykorzystaniem mikrokontrolerów DSC.* (***Projekt i symulacje zasilacza średniej mocy i średniej częstotliwości przeznaczonego do procesów plazmowych i rozpylania magnetronowego***)

Abstract. *The article presents a 4th order power converter of LCLC type. The presented solution works with a frequency of about 100 kHz, and the converter is designed to deliver supply to the magnetron. This unpopular topology has an output type that can be characterized as a current source, with the ability to generate high voltage without load, which is advantageous when used with plasma processes. Furthermore, LCLC topology in this application allows the use of slower control circuits, enabling the implementation of digital feedback loops using DSC microcontrollers.*

Słowa kluczowe: przetwornica rezonansowa LCLC, klasa DE, symulator NGSPICE, rozpylanie magnetronowe.
Keywords: LCLC resonant converter, class DE, NGSPICE simulator, magnetron sputtering.

Introduction

Power supplies designed for magnetron sputtering and plasma processes should work with various load conditions, which is hard to conform with high efficiency and stability [1]. Because of the load variations, in the classic power converters, the controller needs to be fast and complicated to maintain power supply parameters in the safe range of currents and voltages.

The proposed method of reducing the bandwidth of the power converter controller is to use LCLC topology [2]. LCLC converters are used to drive LEDs modules, fluorescent lamps, and many others [3][4].

In LCLC topology, the output power is controlled by adjusting the switching frequency. LCLC converters can achieve high efficiency due to zero voltage switching (ZVS) [5]. Another advantage is that it behaves like a current source, so it can work in the short circuit condition without damage and provide high voltage at the startup. However, this topology also has many drawbacks like high order of transfer function from control to output [2], giving additional control problems [6]. Additionally, compared to simple LC circuits, more magnetic components cause increased power losses. Single integrated magnetic elements can integrate the main inductor and transformer [7] into a single element, reducing power losses in the core.

Due to the 4th order of circuit transfer function, it is hard to control output parameters for stability under various load conditions. Non-linearity is another problem.
There are no dedicated LCLC integrated controllers, and the tailoring of the other resonant converter for this case is very complicated. One of the possibilities is to use DSC (Digital Signal Controller) microcontrollers [8] to simplify the development of non-linear regulators. Such converters can work well enough to maintain stability with a simple digital PI (Proportional-Integrate) controller [9].

Power converter

A power converter is created as an LCLC circuit with an integrated quality factor limiter [10]. The simplified block diagram is presented in Figure 1.

The circuit contains a half-bridge, which drives the LCLC tank. It includes two separate magnetic elements, L1 and L2. The inductance of inductor L1 is essential to limit current during a short circuit at the output. This inductance can be included in a transformer as a leakage inductance. However, in this project, the value must be high and easily changeable due to the prototype nature of this design.

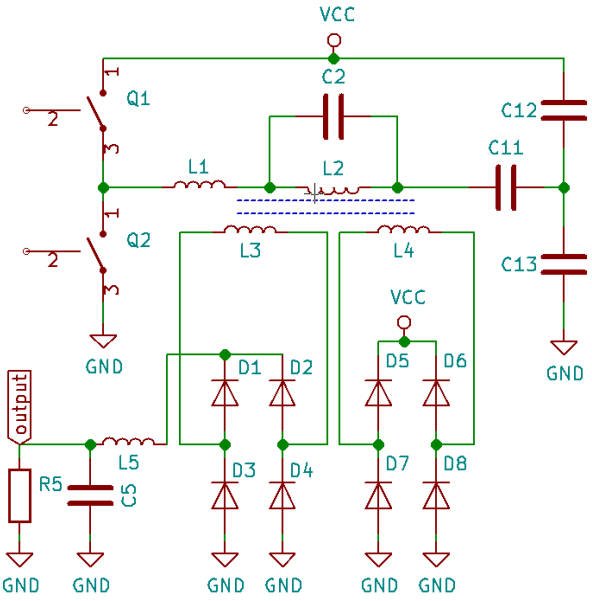

Fig. 1. Simplified schematic of LCLC converter with output rectifier.

When such LCLC tank is used without an output rectifier, the resonant frequency is changed when the load is connected directly to the resonant tank. In that case, the controller must react to these changes by measuring load impedance by fast changes of switching frequency. With a full bridge rectifier, the control can be simplified because the rectifier reduces this influence.

An essential part of the design is to select inductors and capacitances values correctly to achieve acceptable values of voltages and currents with various loads. The best outcome would be to achieve small capacitances and inductances to provide low losses and dimensions.

The selected values of selected elements used in the simulation are presented in Table 1.

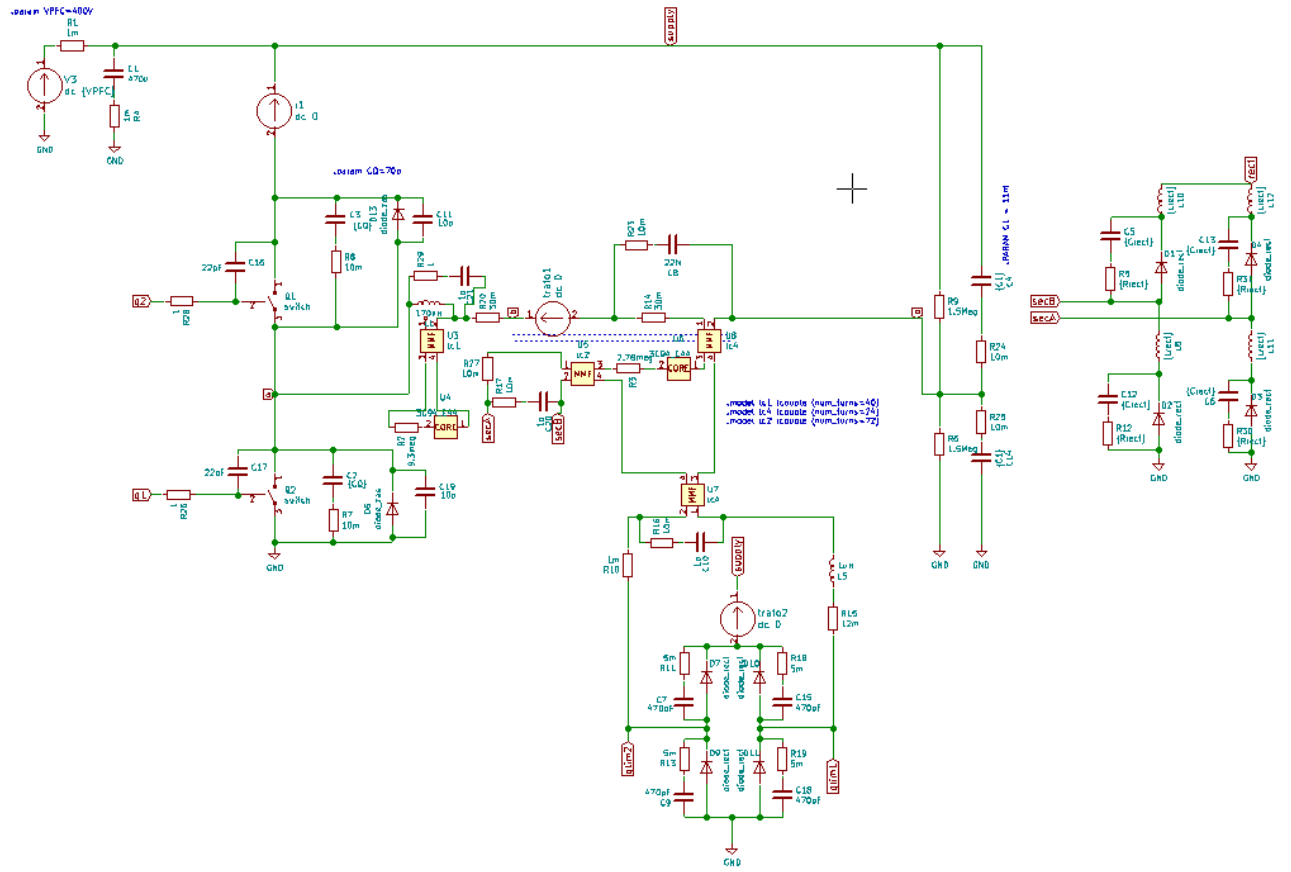

Fig. 2. Simulation schematic of the LCLC power converter with quality factor limiter

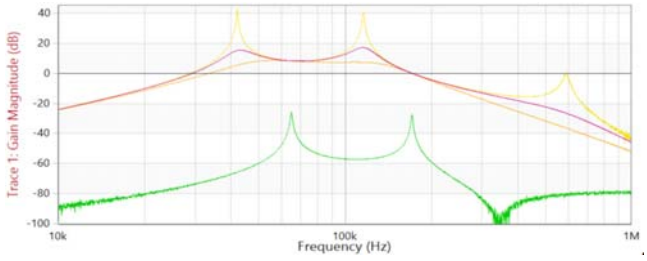

Fig. 3. Measured gain of LCLC tank, Yellow - no load, Green- short circuit, Orange – 470 Ω, Red - 1.5 kΩ

Table 1. Ideal calculated and simulated LCLC tank values

Element	Inductance
L1	170 μH
L2	200 μH
L3	1800 μH
C12, C13	13.1 nF
C2	26.2 nF

Simulations

The schematic was created in iterations. The first version of the DC-DC converter was done with ideal, theoretical elements and further improved by incorporating parasitics.

Simulations were made with calculated values, then improved by further simulations. Finally, the board and LC tank were created and then measured, and the simulation schematic was updated with new values. Furthermore, a comparison was made.

The simulation circuit is presented in Figure 2. Schematics are created with KiCad, and simulations are made with the NgSpice simulator.

The circuit contains a half-bridge with the simplified model of GaN transistors, which were selected for testing purposes. Half-bridge drives LCLC resonant tank with inductors simulated with the usage of reluctance models. The right side presents a full bridge rectifier; the bottom part shows a quality factor limiter.

The frequency operating range of the converter varies from 130 kHz to 200 kHz. It is considered slow for such fast transistors, but the aim was to test a new solution. Figure 3 shows a gain of the LCLC tank circuit. Input is a switching point of half-bridge; output is measured before a rectifier. The operating frequency range is always above second resonance to maintain zero voltage switching, protecting transistors, and reducing losses.

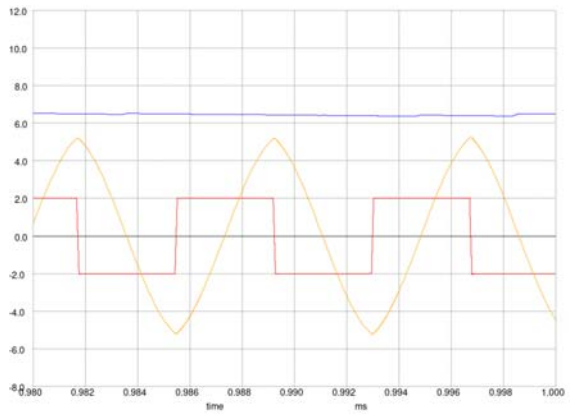

Fig. 4. Simulations with no load condition, Red - half-bridge output (200 V/div), Blue - output voltage (200 V/div), Yellow - half-bridge current (2 A/div). Supply: 400 V, Output voltage peak: about 650 V, Current amplitude: 5A

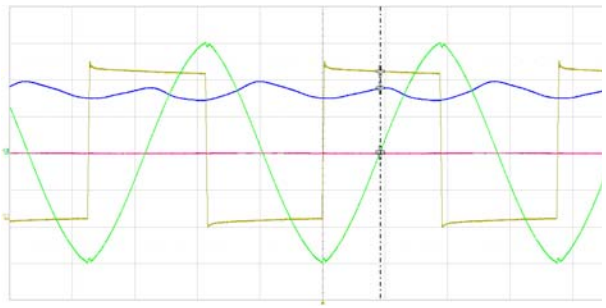

Fig. 5. Measurements with no load condition. Switching frequency: 133 kHz, Yellow - half-bridge output (100 V/div), Blue - output voltage (500 V/div), Green - half-bridge current (2 A/div). Supply: 400 V, Output voltage peak: almost 1 kV, Current amplitude: 6 A

Simulation results are presented in figures 4,6,8. Tests are made for no-load, short circuit, 220 Ω conditions.

Waveforms show essential voltages and currents, such as half-bridge voltage, current, output voltage, and short circuit output current.

Measurements

Measurements were made using the PCB shown in Figure 10. This board is a physical representation of the simulation schematic. Inductances of magnetic elements are presented in Table 2. and measured using OMICRON Bode 100.

Table 2. Measured LCLC tank values at 140 kHz.

Element	Inductance
L1	169.5 μH
L2	212.5 μH
L3	1809 μH

Waveforms are presented in Figures 5, 7, 9. Comparison between simulation and measurements for the no-load condition is presented in Figure 4 and Figure 5. In a physical circuit, the output voltage peak is larger than in comparison to simulation, but the current amplitude is similar.

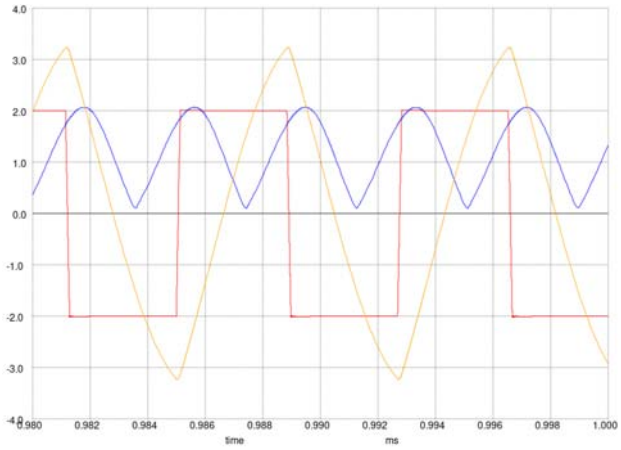

Fig. 6. Simulation with 220 Ω load, Red - half-bridge output (100 V/div), Blue - output voltage (100 V/div), Orange - half-bridge current (1A/div). Supply: 400 V, Output voltage peak: 200 V, Current amplitude: 3.2 A

Load with 220 Ω resistance is shown in Figure 6,7. In that case, the output voltage peak is similar, but in a physical circuit, the voltage does not drop to zero as in simulation. It is caused by capacitances that are not considered in almost ideal models used in the simulation. The shape of the current waveform is similar, but the amplitude in the physical circuit is smaller.

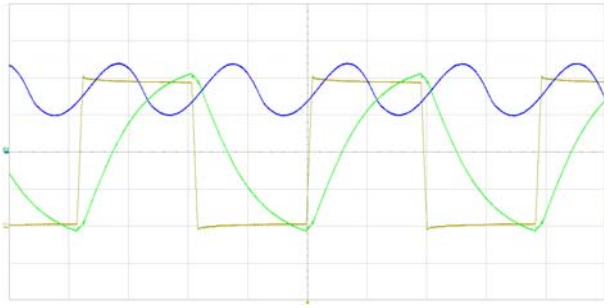

Fig. 7. Measurement with 220 R load. Switching frequency: 130 kHz, Yellow - half-bridge output (100 V/div), Blue - output voltage (100 V/div), Green – half-bridge current (1 A/div). Supply: 400 V, Output voltage peak: 240 V, Current amplitude: 2.0 A

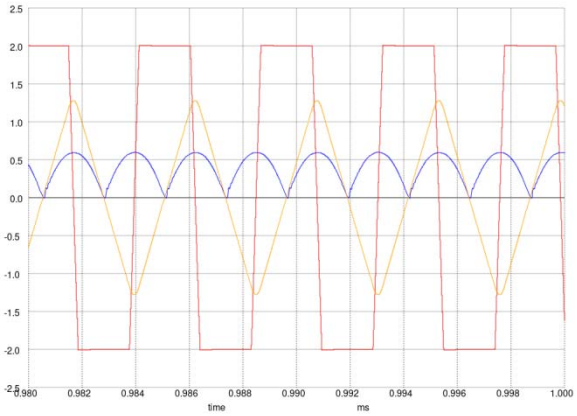

Fig. 8. Short circuit simulation. Red - half-bridge output (50 V/div), Blue - output current (500 mA/div), Green – half-bridge current (500 mA/div). Supply: 400 V, Half-bridge current amplitude: 1.3 A, Output current peak: 550 mA,

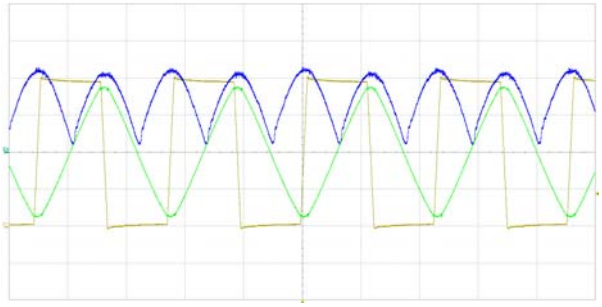

Fig. 9. Short circuit measurements. Switching frequency: 220 kHz, Yellow - half-bridge output (100 V/div), Blue - output current (200 mA/div), Green – half-bridge current (1 A/div). Supply: 400 V, Half-bridge current amplitude: 1.8 A, Output current peak: 400 mA.

The last test was performed in the short-circuit condition. The situation is presented in Figures 8, 9. In this case, waveforms are very similar between simulation and measurement. However, the half-bridge current is greater in the physical circuit. The short circuit current in simulation is slightly higher, probably due to the not correctly modeled resistances used in simulation models and different losses.

Tests also show that using NV6117 Gan transistors with an integrated driver shows some difficulty. When there is no load, the temperature of elements rises to about 100 degrees Celsius, but when the converter is loaded with a full load and currents are much higher, the temperature drops significantly. Measurements are made with a thermocouple by contact with the case. The situation does not depend on the dead-time, and there are no oscillations

observable with accessible equipment. ZVS is present, and output waveforms are perfect. The change of switching slope also does not solve the problem, and the simulation with different parasitic also does not show anything significant. The issue also cannot be observed with GaN simulation transistor models from the producer.

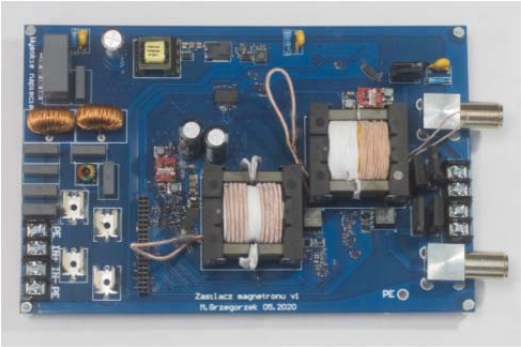

Fig. 10. Picture of the test board used for measurements

Conclusions

Presented LCLC topology has benefits in magnetron sputtering due to current source output. It allows creating high voltages under no-load conditions. The output voltage can also be controlled by switching frequency changes, allowing to ignite the plasma. When plasma is created, the current rises and the converter automatically reduces voltage due to current stabilization. The feedback loop constantly monitors and controls output current. Furthermore, the quality factor limiter, which works as a lossless resistor, protects the circuit from too high voltages when an immediate change of load occurs too fast for controller possibilities.

Simulations have shown that the usage of this topology seems to be a viable solution, and hardware measurements confirm this. However, a comparison of simulation and measurements indicates that there are observable differences. To achieve more accurate results in simulation, much more complicated models of magnetic elements are necessary. The most essential and complex task is a modeling of the losses in magnetic elements. The attempts with the NV6117 GaN transistor have shown a problem with internal losses at no-load conditions. In conclusion, the usage of SiC transistors in such circuits is more reasonable.

Further improvements can be made to the LCLC design by using other SiC or GaN transistors. Other enhancements include creating more accurate simulations by modeling magnetic element losses and using more parasitic elements.

This work was supported by AGH University of Science and Technology, grant no. 16.16.230.434. Special thanks to Michał Grzegorzek for the design and assembly of the PCB board.

***Autorzy**: mgr inż. Mateusz Zapart, AGH University of Science and Technology, al. Adama Mickiewicza 30, 30-059 Kraków, E-mail: mzapart@agh.edu.pl; dr hab. inż. Cezary Worek, AGH University of Science and Technology, al. Adama Mickiewicza 30, 30-059 Kraków, E-mail: worek@agh.edu.pl .*

LITERATURA

[1] Sarakinos K., Alami J., Konstantinidis S., High power pulsed magnetron sputtering: A review on scientific and engineering state of the art, Surface and Coatings Technology, (204) 2010, n.11, 1661-1684

[2] Y. Aug, M. P. Foster, C. M. Bingham, D. A. Stone, H. I. Sewell and D. Howe, Analysis of 4th-order LCLC Resonant Power Converters, IEE Proc. Electric Power Applications, (15)2004, 169-181

[3] Khatua M., Kumar A.,Dragan M., Khurram K. A., A High-Frequency LCLC Network Based Resonant DC-DC Converter for Automotive LED Driver Applications, 19th Workshop on Control and Modeling for Power Electronics (COMPEL), 2018

[4] Ang Y-A, Stone D., Bingham C., Foster M., Rapid Analysis & Design Methodologies of High-Frequency LCLC Resonant Inverter as Electrodeless Fluorescent Lamp Ballast, 7th International Conference on Power Electronics and Drive Systems, 2007

[5] Bin Z.., Gang W., Dong L. W.,. Analysis and design of the Resonant Current of the LCLC Resonant Converters with Consideration of Zero-Voltage Switching and Zero-current Switching, Journal of Microwave Power and Electromagnetic Energy, (32) 1997 n.1, 28-33

[6] Widorek R., Worek C., Sequential cycle stealing – a novel control method dedicated for resonant converters, 17th European Conference on Power Electronics and Applications, 2015

[7] Worek C., Ligenza S., Zintegrowany element magnetyczny zwiększający sprawność rezonansowych układów przetwarzania energii, Przegląd Elektrotechniczny, (88) 2012, n.11b, 323-325

[8] Sheng B., Chen Y., Wang H., Liu Y-F, Sen P.C., High Efficiency Wide Input Voltage Range LCLC Resonant Converter Using Nonlinear Frequency Controller, IEEE Energy Conversion Congress and Exposition (ECCE), 2018

[9] Zheng S., Czarkowski D., Modeling and Digital Control of a Phase-Controlled Series–Parallel Resonant Converter, IEEE Transactions on Industrial Electronics, 54 (2007) No. 2, 707-715

[10] Zapart M., Worek C., A mixed-mode analog-digital simulation of LLC resonant power converter with the quality factor limiter", Przegląd Elektrotechniczny, (97) 2021 nr. 2, 82-86